

## EVALUATION OF TOPCON TECHNOLOGY ON LARGE AREA SOLAR CELLS

F. Feldmann<sup>1,2,\*</sup>, B. Steinhauser<sup>1</sup>, V. Arya<sup>1</sup>, A. Büchler<sup>1</sup>, A. A. Brand<sup>1</sup>, S. Kluska<sup>1</sup>, M. Hermle<sup>1</sup>, S. W. Glunz<sup>1,2</sup>

<sup>1</sup>Fraunhofer Institute for Solar Energy Systems (ISE), Heidenhofstrasse 2, 79110 Freiburg, Germany

<sup>2</sup>Department of Sustainable Systems Engineering (INATECH), Albert-Ludwigs University Freiburg, Georges-Köhler-Allee 103, 79110 Freiburg, Germany

\*Corresponding author: frank.feldmann@ise.fraunhofer.de, +49 (0) 761 4588 5287

**ABSTRACT:** Passivating contacts, like TOPCon or poly-Si/SiO<sub>x</sub>, have pushed the efficiency of crystalline silicon (c-Si) solar cells notably. Currently, the world-record efficiency of 25.7% for a both-sided contact solar cell has been achieved by an n-type solar cell featuring a selective boron front emitter and a passivating rear contact (TOPCon). Like the 25%-efficient PERL cell, this record cell was realized on a small area of 2x2 cm<sup>2</sup> using lab processes, like photolithography and evaporation of metal contacts. This paper addresses the first steps towards the realization of a large area TOPCon cell by industry-relevant fabrication steps. The scope of this paper lies on the application of laser ablation and NiCu plating to a 1.5µm deep, 140 Ω/sq boron-diffused emitter. The 10x10 cm<sup>2</sup> cell yielded an efficiency of 22.9%.

**Keywords:** n-type, Silicon Solar Cell, Passivation, PECVD

### 1 INTRODUCTION

Passivating and carrier-selective contacts which consist of an ultrathin SiO<sub>x</sub> layer and a heavily doped silicon film (e.g. TOPCon [1] or poly-Si [2, 3]) are an appealing technology to further push the efficiency of silicon solar cells. The replacement of a partial rear contact (PRC) scheme by TOPCon as a full-area rear contact has so far resulted in efficiencies up to 25.7% [4]. The potential of such an approach has been shown only on an area of 2x2 cm<sup>2</sup>. The first solar cells of practical size (≥100 cm<sup>2</sup>), which featured a passivating rear contact and a diffused front side, however, achieved efficiencies of only 20.7% [5] and 21.2% [6]. Both solar cells were -amongst other things- strongly limited by recombination at the front side and, therefore, did not benefit from the excellent surface passivation enabled by the passivating rear contact.

In this paper, we demonstrate 100 cm<sup>2</sup> n-type solar cells featuring a homogeneous boron emitter and a passivating rear contact. The scope of this paper lies on the formation of the front grid using laser contact opening (LCO) and NiCuAg plating.

### 2 EXPERIMENTAL DETAILS

#### 2.1 Fabrication of large area solar cells

Solar cells of significant area (10x10 cm<sup>2</sup>) were fabricated on shiny-etched, 1 Ωcm n-type float-zone silicon. The cell layout is shown in Fig. 1. On the front random pyramids were formed by alkaline texturing and a 140 Ω/sq emitter ( $N_{\text{surf}} = 1 \times 10^{18} \text{ cm}^{-3}$ , depth = 1.5 µm) was realized by tube furnace diffusion and subsequent drive-in oxidation. At the rear, the TOPCon structure was applied as described in Ref. [1]. The front surface was passivated by a stack of Al<sub>2</sub>O<sub>3</sub> and SiN<sub>x</sub>. The front contact openings were realized by laser ablation using a UV/ps laser source. Thereafter, the front and rear surface passivation were activated using an atomic hydrogen treatment (RPHP) [7] at 425 °C. The rear contact was formed by thermal evaporation of Ag and the front grid was realized by forward bias plating of Ni, Cu, and Ag. Finally, a second anti reflection layer was applied at the front by evaporation of MgF<sub>2</sub>.

#### 2.2 Characterization and analysis

The minority carrier recombination at the laser-formed contact openings ( $J_{0,\text{LCO}}$ ) was investigated on a symmetric passivated  $J_{0e}$  sample using lifetime calibrated photoluminescence imaging (PL).

The light and dark  $I$ - $V$  characteristics of the solar cells were measured using the LOANA setup from pv-tools. To further

analyse the performance of the solar cells, 3D device simulations using Quokka v3 were performed. The input parameters, e.g.  $J_{0e}$ ,  $J_{0,\text{LCO}}$ , were determined from  $J_{0e}$  samples.

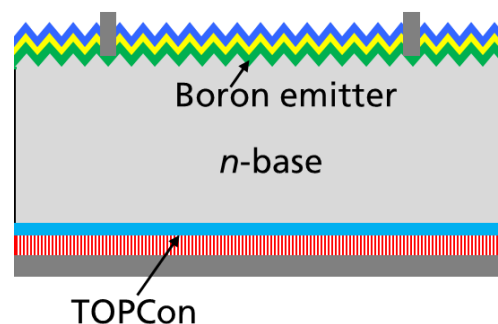


**Figure 1:** Solar cell structure featuring a homogeneous boron emitter and n-TOPCon as passivating rear contact.

### 3 RESULTS

#### 3.1 Laser contact opening

The influence of the laser contact opening (LCO) process was determined as a function of laser power on a symmetric boron-diffused and passivated  $J_{0e}$  sample. The corresponding PL image after single-sided LCO is depicted in Fig. 2. The sample's total  $J_0$  (including the bulk) before laser averaged to 46.2 fA/cm<sup>2</sup> which resulted in  $J_{0e} = 18.1 \text{ fA/cm}^2$  for either side. After LCO the total  $J_0$  was significantly increased, especially for the highest used laser power  $J_0$  increased by a factor of more than 3. This corresponds to a  $J_{0,\text{LCO}} > 10000 \text{ fA/cm}^2$  (calculated with ~0.4% contact opening). On the other hand, for the two lowest laser powers the total  $J_0$  increased only to 59 fA/cm<sup>2</sup> and 62 fA/cm<sup>2</sup>, respectively. The corresponding  $J_{0,\text{LCO}}$  were 2700 fA/cm<sup>2</sup> and 3300 fA/cm<sup>2</sup>, respectively.

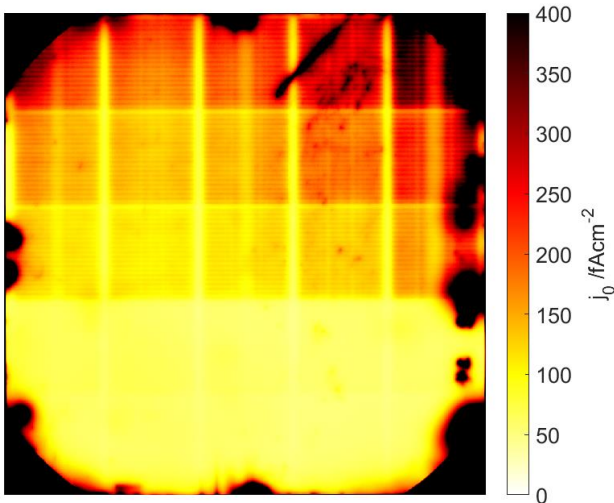


**Figure 2:** PL image of a  $J_{0e}$  sample after LCO. The upper row was subjected to the highest laser power, while the lower row was subjected to a tenth of the maximum laser power.

These values were used to calculate the  $V_{oc}$  as a function of the metallized area fraction. The dashed line refers to the calculation with  $J_{0,LCO} = 3300 \text{ fA/cm}^2$  and the solid lines refer to the ideal case, wet-chemical contact opening which does not introduce damage to the crystal ( $J_{0,WCO}$ ). Using 1D device simulations [8]  $J_{0,CO} = 1800 \text{ fA/cm}^2$  was determined. Since  $J_{0,LCO}$  is higher than  $J_{0,WCO}$  the  $V_{oc}$  is expected to be lower when using LCO instead of wet-chemical contact opening. With  $A_{\text{metal}} \approx 1.2\%$ , a  $V_{oc}$  of about 695 mV is expected.

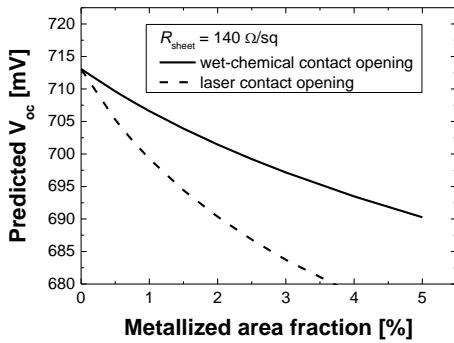


**Figure 3:**  $V_{oc}$  as a function of metallized area fraction for the  $140 \text{ } \Omega/\text{sq}$  emitter. The solid line refers to wet-chemical contact openings, which do not damage the crystal and the dashed line refers to LCO, which induces certain crystal damage.

### 3.2 Solar cell results and analysis

The solar cell results for the best cell are shown in Table I. The  $V_{oc}$  of 694 mV matched very well the calculation shown in Fig. 3 and showed that the influence of the laser contact opening was well estimated. The FF and pFF values were 81.0% and 83.9%, respectively. The pFF was slightly lower than the ideal  $FF_0$  (84.6%) as the laser-induced damage probably affected the cell at maximum power point conditions, too. From the difference between pFF and FF the series resistance was calculated to  $R_s = 0.58 \text{ m}\Omega\text{cm}^2$ . In order to measure the contact resistivity of the fingers by the TLM method, multiple solar cells were diced into stripes. The contact resistivity of the metal fingers averaged to  $\rho_c = 0.53 \pm 0.19 \text{ m}\Omega\text{cm}^2$  and, therefore, did not affect the FF significantly. Instead, a FF loss of  $1\%_{\text{abs}}$  can be attributed to the grid resistance. This is supported by the

measurement of the grid resistance (busbar to busbar) which revealed a resistance of  $80 \text{ m}\Omega$ , amounting to approx. one third of  $R_s$ .

The  $J_{sc}$  was  $40.8 \text{ mA/cm}^2$ . Due to a metal coverage of  $\sim 2\%$ , the main  $J_{sc}$  loss can be attributed to shading by the front metal grid. The influence of ghost plating was present but is yet to be quantified.

In total an efficiency of 22.9% was measured. Fig. 4 shows the free energy loss analysis (FELA) obtained from the numerical device simulation. It can be clearly seen that there are two dominant loss mechanisms. The resistive loss incurred by the grid fingers has a share of  $\sim 32\%$  of the total loss. The aggregate loss due to recombination in the emitter (including contacted regions) takes a similar share of  $\sim 34\%$  of the total energy loss. Hence, the simulation reveals that both the LCO and plating process have the highest potential for improvement.

**Table II:** Light  $I$ - $V$  results of  $10 \times 10 \text{ cm}^2$  n-type solar cell.

Cell	$V_{oc}$ [mV]	$J_{sc}$ [mA/cm <sup>2</sup> ]	FF [%]	pFF [%]	$\eta$ [%]
Best	694	40.8	81.0	83.9	22.9

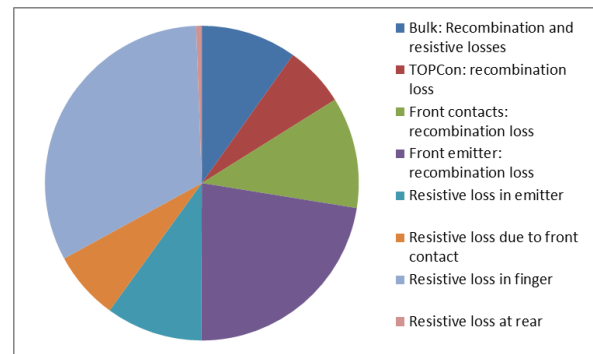


**Figure 4:** Pie chart showing the individual losses of the FELA.

## 4 SUMMARY

$10 \times 10 \text{ cm}^2$  solar cells with homogeneous boron emitter and passivating rear contact were realized. Firstly, the impact of laser ablation on the  $J_0$  was studied and it was found that a low laser power has to be used in order to contain crystal damage. Still, the Si crystal was damaged during LCO, which resulted in a significant increase of the recombination current ( $J_0$ ) at the metal front contacts. Secondly, solar cells featuring NiCu plated front metallization were realized and analyzed. An efficiency of 22.9% was measured. The FELA revealed that the dominant losses were the limited finger conductivity and the minority carrier recombination at the front side. From literature it is known that laser damage can be cured by forming gas annealing or firing [9]. Alternatively, the threshold energy for ps laser ablation can be reduced by using a nanosecond pre-pulse thereby mitigating the impact of laser damage significantly [10]. Hence, future work will focus on a “damage-free” laser process and an optimized front metallization with respect to shading and conductivity.

## 5 ACKNOWLEDGMENTS

The authors would like to thank A. Leimenstoll, F. Schätzle, A. Seiler, and S. Seitz for processing of the solar cells in the cleanroom and G. Cimiotti is thanked for plating the solar cells. Furthermore, the authors acknowledge F. Martin and E. Schäffer for measuring the  $I$ - $V$  characteristics of the solar cell.

This work was funded by the German Federal Ministry for Economic Affairs and Energy under contract number 03225877D (PROJECT PEPPER).

## 6 REFERENCES

- [1] F. Feldmann, M. Bivour, C. Reichel, M. Hermle, and S. W. Glunz, *Solar Energy Materials and Solar Cells* 120 (2014) 270.
- [2] U. Römer, R. Peibst, T. Ohrdes, B. Lim, J. Krügener, E. Bugiel, T. Wietler, and R. Brendel, *Solar Energy Materials and Solar Cells* 131 (2014) 85.
- [3] D. Yan, A. Cuevas, J. Bullock, Y. M. Wan, and C. Samundsett, *Solar Energy Materials and Solar Cells* 142 (2015) 75.
- [4] A. Richter, J. Benick, F. Feldmann, A. Fell, M. Hermle, and S. W. Glunz *Solar Energy Materials & Solar Cells* to be published (2017)
- [5] M. K. Stodolny, M. Lenes, Y. Wu, G. J. M. Janssen, I. G. Romijn, J. R. M. Luchies, and L. J. Geerligs, *Solar Energy Materials and Solar Cells* 158 (2016) 24.
- [6] Y. G. Tao, V. Upadhyaya, C. W. Chen, A. Payne, E. L. Chang, A. Upadhyaya, and A. Rohatgi, *Progress in Photovoltaics* 24 (2016) 830.
- [7] S. Lindekugel, H. Lautenschlager, T. Ruof, and S. Reber, in *Proceedings of the 23rd European Photovoltaic Solar Energy Conference, Valencia, Spain, 2008*, p. 2232.
- [8] K. R. McIntosh and P. P. Altermatt, *35th Ieee Photovoltaic Specialists Conference* (2010) 2188.
- [9] A. Uruena, M. Aleman, E. Cornagliotti, A. Sharma, M. Haslinger, L. Tous, R. Russell, J. John, F. Duerinckx, and J. Szlufcik, *Progress in Photovoltaics* 24 (2016) 1149.
- [10] A. A. Brand, F. Meyer, J. F. Nekarda, and R. Preu, *Applied Physics a-Materials Science & Processing* 117 (2014) 237.